

Methods of workspace generation for parallel kinematic manipulators

Wesley Dharmalingum^{1*}, and Jared Padaychee¹

¹Discipline of Mechanical Engineering, School of Engineering, University of KwaZulu-Natal, South Africa

Abstract. This paper presents the geometric, discretization and Monte Carlo method to generate the workspace for Parallel Kinematic Manipulators (PKMs). The geometric method does not require the solution to the inverse kinematics as opposed to the Monte Carlo and discretization methods. Each method possesses advantages and drawbacks concerning accuracy, time and ease of implementation. A case study concerning constant orientation workspace of a planar 3RRR PKM showed that the most efficient and accurate method was the geometric method but it also possessed the most limitations. The discretization and Monte Carlo methods produced the workspace with an accuracy of 92.49% and 95.67% respectively.

1 Introduction

Parallel Kinematic Manipulators (PKMs) are comprised of at least two closed loop kinematic chains that connect a robot's base to its end effector. PKMs possess a high payload capacity, high accuracy and are capable of achieving high speeds [1]. Some drawbacks of PKMs include complex calibration, complex forward kinematic analysis and smaller workspaces in comparison to serial robots [2]. There exist different types of workspace that are defined according to an operating point, usually on the end effector, reaching viable locations and whilst considering the orientation of the end effector at these viable points. Establishing the workspace of a robotic manipulator is an important task that precedes path planning. Robot characteristics can also be assessed within a particular workspace during the design phase [3]. Such robot characteristics include, stiffness, dexterity transmission quality, etc. Geometric, discretization and numerical methods are three general methods that can be adopted to establish the workspace of a robotic platform [4].

The geometric method involves the analyses of the geometric design parameters of the robot and the motion profiles of the robot's links and joints. Usually, the intersecting areas or volumes produce the boundaries of the workspace. The geometric method was used by Le and Le [5] to generate the equations that defined the workspace of a RUU Type Delta PKM. Li and Angeles [6] developed a novel PKM called the SDelta and employed the geometric method to generate the workspace. The PKM was shown to offer a large workspace. This

* Corresponding author: DharmalingumW@ukzn.ac.za

method was also used by Moldovan [7] to generate vertical and horizontal cross-sections of the workspace for the 6-PGK PKM. Ay et al. [8] used the forward and inverse kinematic analyses to develop a novel geometric approach for the workspace analysis of a spatial PKM. Merlet et al. [9] investigated different types of workspaces of planar PKMs and presented the associated geometric algorithms. Concerning optimum design and PKM accuracy comparison, Yu et al. [10] developed a geometric approach to determine position and orientation angle errors due to actuators inaccuracies. This method was only applied to planar 3-DOF PKMs that were fully parallel and possessed singularity free workspaces.

The discretization method converts a region in space to a set of nodes. Each node is then tested using the inverse kinematic analysis describing a particular PKM. If the mechanical constraints are satisfied, the point is considered as part of the workspace. Peidro et al. [3] adopted the discretization method based on the forward and inverse kinematics to obtain the external and internal workspace boundaries respectively. Due to the robotic platform being a redundant serial-parallel robot, the forward and inverse kinematics were used. Monsarrat and Gosselin [11] developed the workspace of a 6-DOF PKM and then performed a workspace-based kinematic optimisation. The discretization method was successfully adopted. In a study conducted by Lou et al. [12] investigated the optimal design of the Delta PKM and the Stewart-Gough platform. The workspace shape and quality were presented which involved discretization of the regular workspace. Russo and Ceccarelli [13] generated the workspace of the CaPaMan and 3-UPR PKM architectures using the geometric and discretization approach. The study showed that the geometric approach produced the workspace faster than the discretization method but could not provide any information concerning the self-collision constraints. Stan et al. [14] investigated the performance characteristics of a Delta PKM and implemented the discretization method. The performance of the PKM was evaluated throughout the established workspace.

The Monte Carlo method is a numerical method that involves repeated random sampling to generate points which are checked against the inverse kinematics of a PKM. Like the discretization method, if a point satisfies the robot constraints, it forms part of the robot's workspace. Kuznetcova et al. [15] investigated the use of a haptic device to aid the control of a 4 Degree of Freedom (DOF) PKM and employed the Monte Carlo method for workspace generation. Chaudhury and Ghosal [16] used the Monte Carlo method together with a gradient based optimisation algorithm to investigate PKM optimisation. The study was successfully demonstrated on two PKMs. In another study aimed at optimization, the Delta robot was studied for a given workspace which involved the use of the Monte Carlo method [17]. Jianjun et al. [18] developed an underwater manipulator and generated its workspace with the Monte Carlo method in conjunction with the Denavit-Hartenberg kinematic analysis. Peidro et al. [19] refined the Monte Carlo approach and presented a Gaussian Growth method demonstrated on a 10-DOF robot. This method first develops an inaccurate seed model of the workspace and then further refines the seed workspace by densifying the workspace. The workspace generated was more accurately than conventional Monte Carlo methods.

This research presents the constant orientation workspace development and analysis for a 3RRR planar PKM to demonstrate the geometric, discretization and Monte Carlo methods. The contribution of this paper is the comparison of each method together with its merits and drawbacks. The remainder of this research paper presents the methodology and results in Section 2 and Section 3 presents the conclusions of the study.

2 Methodology and Results

The following sub-sections present the description of the architecture, geometric, discretization and Monte Carlo methods including the procedures and results.

2.1 Description of architecture

The 3RRR PKM, presented in Figure 1, consists of 3 limbs. Each limb possesses 3 revolute joints which are denoted by the letter R. The first revolute joint in each limb is fixed and is also actuated which provides a rotational input to the limbs. The rotational inputs are described by the angles θ_1 , θ_2 and θ_3 . The robot's base is an equilateral triangle defined by points A_1 , A_2 and A_3 . The end effector is also an equilateral triangle and is defined by points C_1 , C_2 and C_3 . Link ℓ_1 is the distance between points A and B whilst ℓ_2 is the distance between points B and C . The links denoted as ℓ_1 and ℓ_2 are referred to as the proximal and distal links respectively. Point P is the midpoint of the end effector. The distance ℓ_3 describes the distance between point C and P . The PKM possesses 3 DOFs which are comprised of translations about the x and y axes and a rotation about the axis normal to the plane of motion denoted as ϕ . The dimensions of the PKM in this study are shown in Table 1.

Table 1. 3RRR PKM dimensions.

Variable	Length (mm)
$A_1A_2 = A_2A_3 = A_1A_3$	235
ℓ_1	100
ℓ_2	135
ℓ_3	69.4

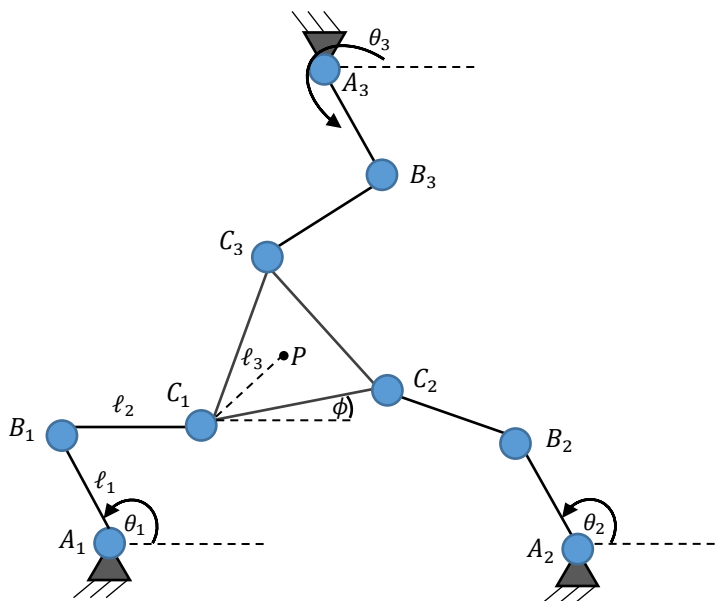


Fig. 1. The 3RRR PKM.

2.2 Geometric method

The geometric method used to develop the workspace for the 3 RRR PKM is based on the research presented in a study by Gosselin and Angeles [20]. The radii of the annular regions swept by each limb is dependent on the lengths ℓ_1 and ℓ_2 . The origin of each radii is dependent on lengths ℓ_1 , ℓ_2 and ℓ_3 , the dimensions of the base and the rotation angle ϕ concerned with the end effector.

2.2.1 Procedure

The workspace was generated using SolidWorks and in conjunction with the geometric method and the procedure is listed below:

- 1) Calculate the inner and outer radii using the variables ℓ_1 and ℓ_2 .
- 2) Calculate the origin for all radii using the variables ℓ_1 , ℓ_2 and ℓ_3 , the dimensions of the base and ϕ . Since the constant orientation workspace is investigated, ϕ is set to zero.
- 3) Draw each circle with radii $|\ell_1 \pm \ell_2|$.
- 4) Delete all sketch elements outside the intersection of the circles.
- 5) Extrude the workspace sketch by any random number
- 6) Measure the area of the bottom or top surface of the SolidWorks part to obtain an accurate measurement of the workspace.

2.2.2 Results

The circles, origins of the circles and their intersecting region is shown in Figure 2. This represents the constant orientation workspace.

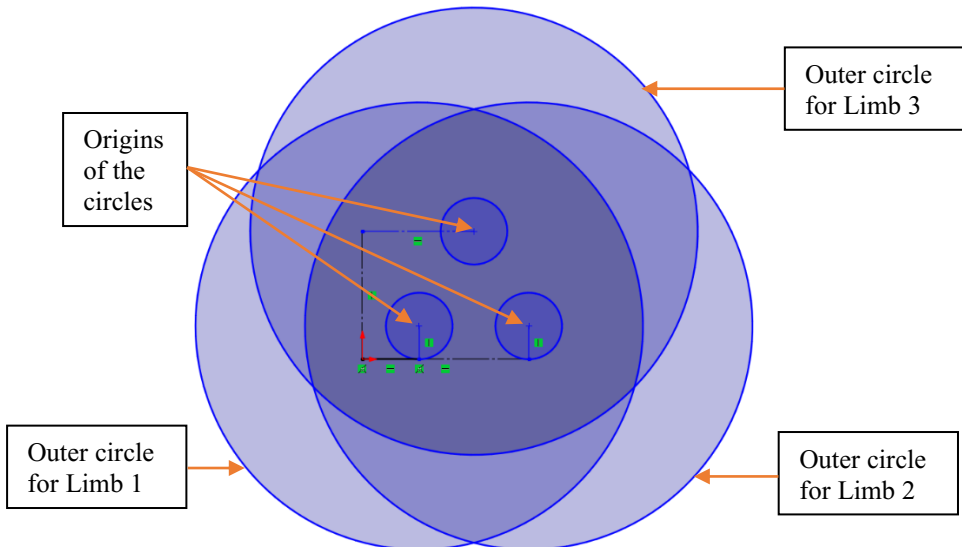


Fig. 2. SolidWorks sketch of the geometric workspace.

The workspace accuracy was confirmed from visual inspections by overlaying the workspace into the assembly model with the 3RRR PKM. Figure 3 shows that the midpoint of the end effector was moved to its extremity on the boundary of the workspace. The midpoint of the end effector was coincident with the boundary-defining arc. The workspace

consists of three boundary arcs and three internal voids. The workspace was evaluated to be 87416.06 mm² and served as a comparison for the discretization and Monte Carlo methods.

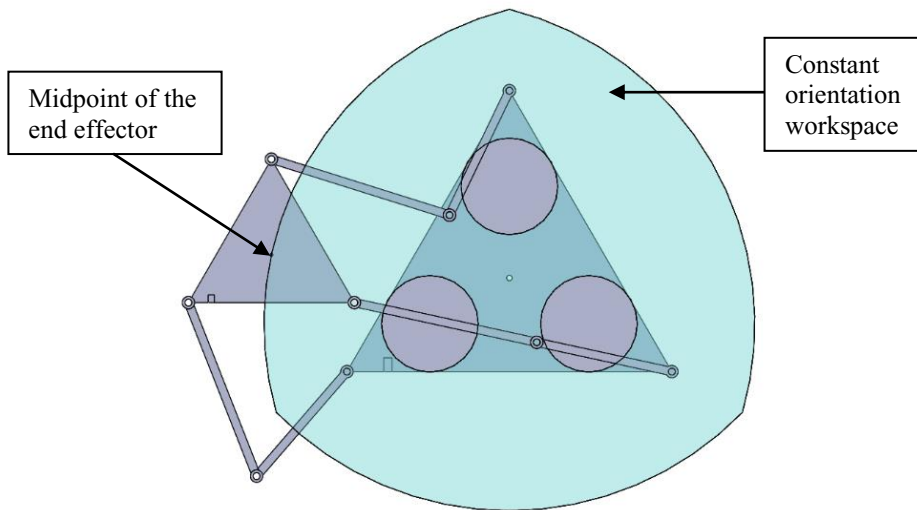


Fig. 3. A visual inspection to confirm the accuracy of the workspace.

2.3 Discretization method

Due to the PKM architectural and workspace symmetry, it was more computationally efficient to discretize one third of the workspace. The discretization was performed using MATLAB®.

2.3.1 Procedure

The procedure to generate the workspace by the discretization method is listed below:

- 1) Establish the x-axis and y-axis upper and lower limits with consideration for symmetry.
- 2) Discretize the workspace using an incremental value along the x and y axes.
- 3) Establish the mechanical constraints of the robotic platform
- 4) Generate points and assess each point against the inverse kinematic solution and mechanical constraints
- 5) Plot all valid points
- 6) Wrap the point cloud with a boundary and determine the size of the wrapped area

Figure 4 depicts the region that was analysed in the aforementioned procedure.

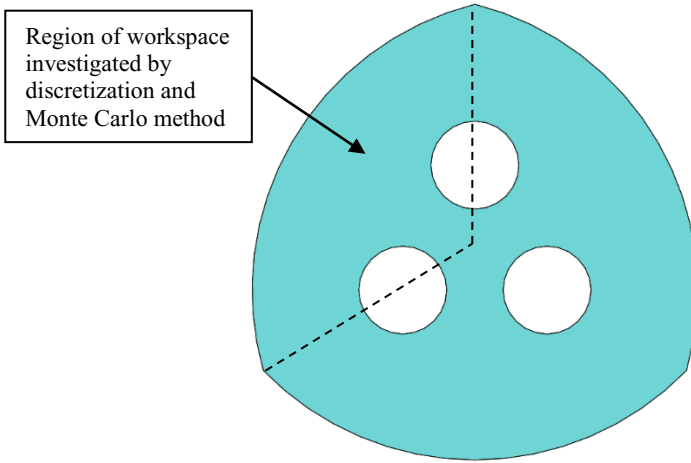


Fig. 4. Region of workspace investigated by discretization and Monte Carlo method.

2.3.2 Results

Figure 5 shows the workspace generated through the discretization method using an increment size of 5 mm. The boundary wrapped around the points is dependent of the shrink factor which determines how tight the boundary is wrapped around the points. A shrink factor of 1 was used and is the most tightly wrapped boundary. The area of the workspace generated was 26950 mm² which is a 92.49% accuracy when compared to the workspace generated by the geometric method.

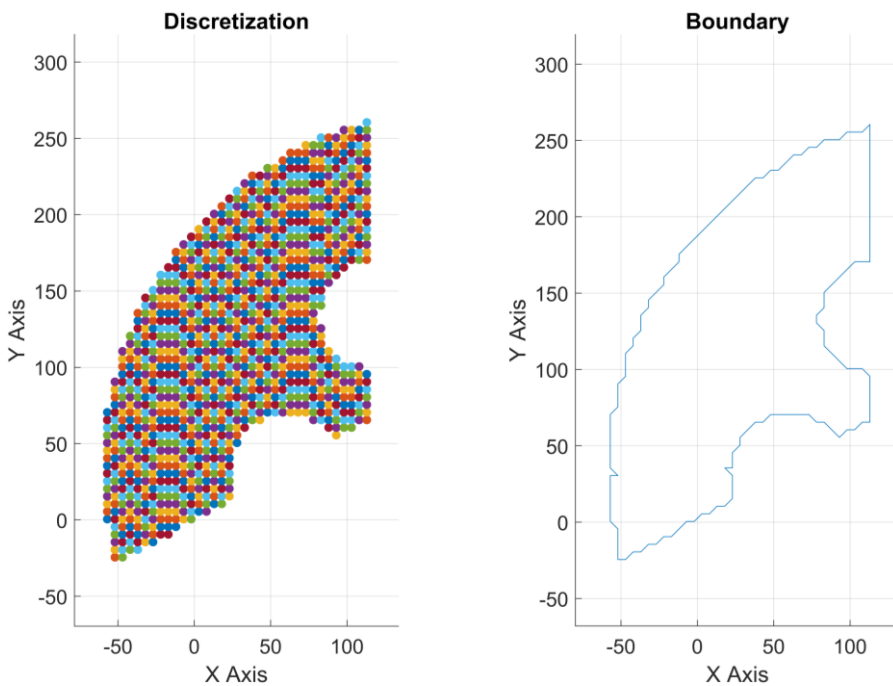


Fig. 5. Increment size of 5 mm and the wrapped boundary with a shrink factor of 1.

Different increment sizes were investigated and is presented in Figure 6. At smaller increment sizes, larger accuracies were observed. The accuracies are with respect to the area generated using the geometric method. Accuracies in the range of 70% were observed for large increments.

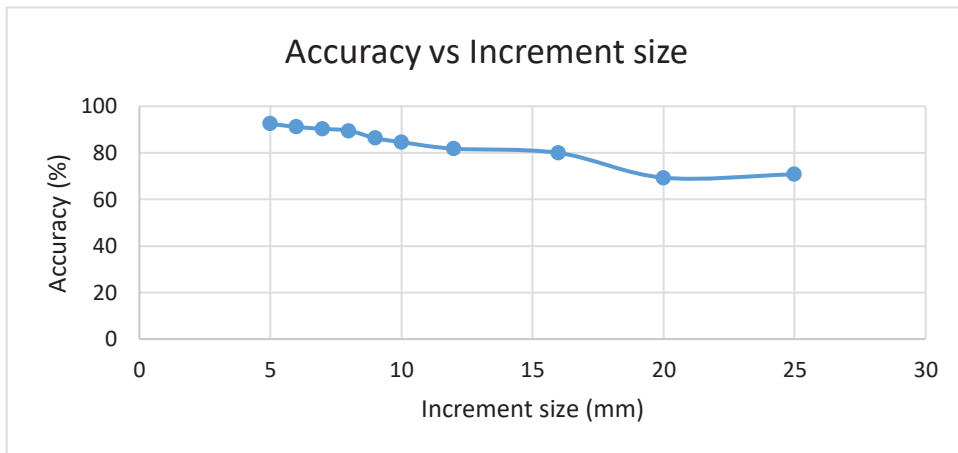


Fig. 6. Graph of accuracy vs increment size for the discretization method.

The influence of increment size on simulation time was investigated. An exponential relationship was observed. At smaller increments, the simulation time is longer than at larger increments. There was a significant decrease in simulation time for an increment size of 9 and larger.

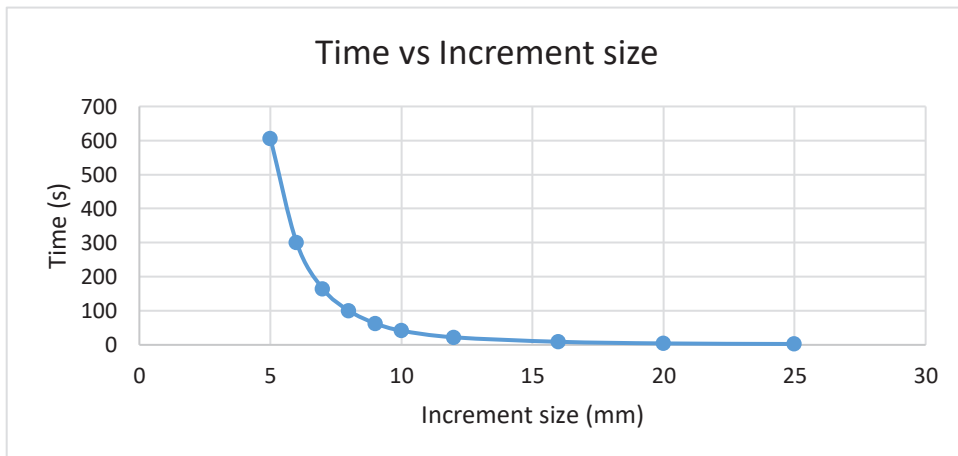


Fig. 7. Graph of time vs increment size for the discretization method.

Figure 8 shows the influence of increment size on the number of points that needed to be assessed by the inverse kinematics to find valid points for the workspace. At smaller increments larger number of points are generated as the region is represented by increased number of nodes. An exponential relationship was observed.

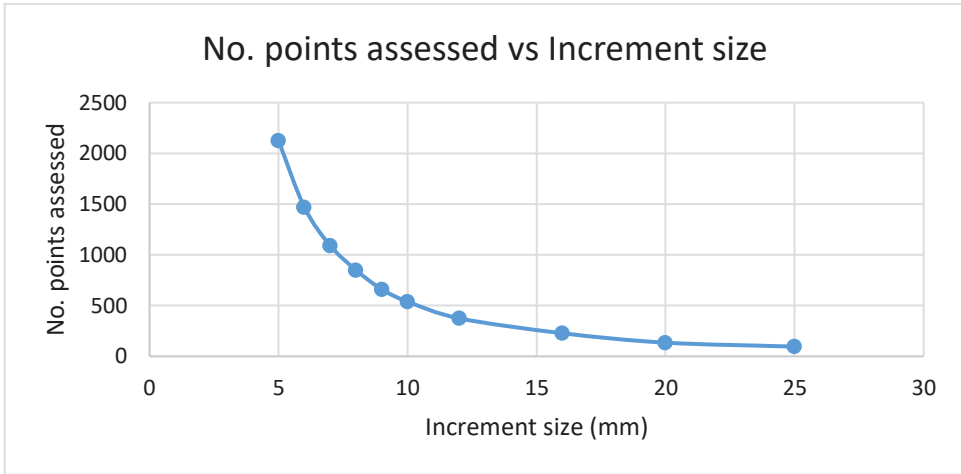


Fig. 8. Graph of number of points assessed vs increment size for the discretization method.

2.4 Monte Carlo method

The workspace generated using the Monte Carlo method was for the region indicated in Figure 4. The Monte Carlo method was performed using MATLAB®.

2.4.1 Procedure

The procedure to generate the workspace by the Monte Carlo method is listed below:

- 1) Establish the x-axis and y-axis upper and lower limits with consideration for symmetry.
- 2) Specify the number of points that must be generated for the point cloud.
- 3) Ensure random numbers are generated between the upper and lower limits.
- 4) Establish the mechanical constraints of the robotic platform
- 5) Assess each point against the inverse kinematic solution and mechanical constraints
- 6) Plot all valid points
- 7) Wrap the point cloud with a boundary and determine the size of the wrapped area.

2.4.2 Results

Figure 9 depicts the workspace generated by the Monte Carlo method. One thousand points were used with a shrink factor of 0.4. The workspace area was 26728 mm². This was an accuracy of 91.73% in comparison to the geometric method. This point cloud was generated in 396 seconds.

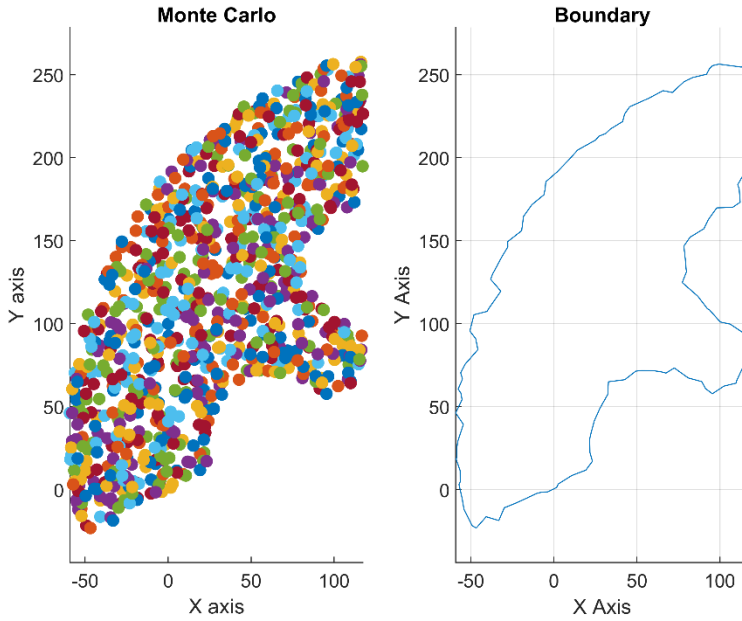


Fig. 9. The Monte Carlo method used to generate 1000 points with a shrink factor of 0.4.

The number of points used to generate the point cloud affects the accuracy of the workspace. Figure 10 shows a general trend that as the point cloud is more dense with points, higher accuracies are achieved.

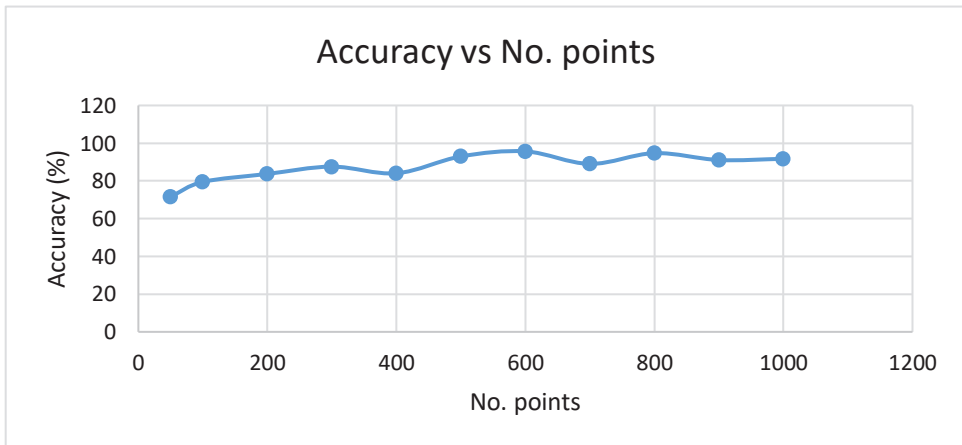


Fig. 10. Graph of accuracy vs number of points for the Monte Carlo method.

The time taken to generate the point clouds were also investigated. An approximate linear relationship was observed between the point cloud density and time to generate the point cloud as seen in Figure 11. More dense point clouds require more time as each point needs to be checked.

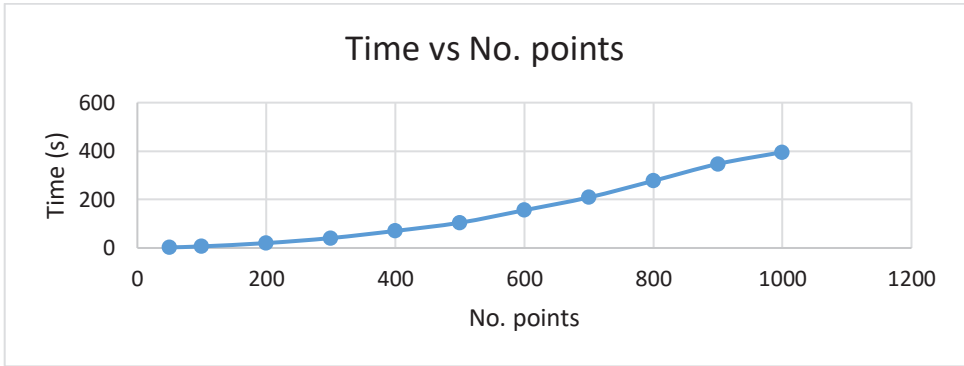


Fig. 11. Graph of time vs number of points for the Monte Carlo method.

Different point clouds were generated with 500 points and a shrink factor of 0.4. This investigation showed that there are differences between the areas generated and this is due to the random coordinates that were generated that do not follow an ordered pattern. The results are seen in Table 2.

Table 2. Variation in results for a point cloud of 500 points and shrink factor of 0.4.

Area (mm ²)	Accuracy (%)	Time (s)
25586	87,80	112,79
27178	93,27	111,91
27079	92,93	120,5
26201	89,91	119,58
26523	91,02	113,61

The point clouds of the first three entries from Table 2 are shown in Figure 12. Regions of less dense points exist in all the point clouds and were in different regions of the workspace. This reaffirms the random patterns of the generated points.

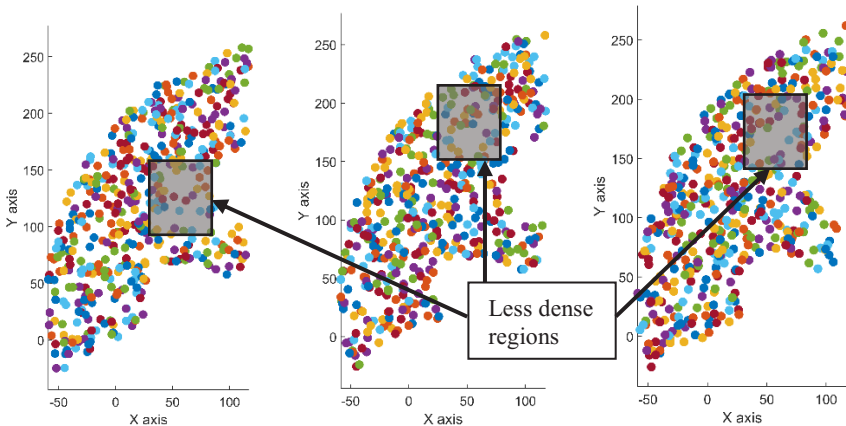


Fig. 12. A comparison of the density of three different point clouds for 500 points with a shrink factor of 0.4.

3 Conclusion

The geometric method was the most efficient and accurate. The geometric method does not rely on the inverse kinematic solution which aids in its use but it cannot be easily adapted for further analysis at specific region of interest in the workspace. This method could also find difficulty in generating complex three dimensional workspaces. The discretization and Monte Carlo methods provided a suitable approximation of the workspace and can be readily adapted for further analyses such as the forward kinematic analysis, singularity analysis and for investigating other machine characteristics. The closest approximations of the discretization and Monte Carlo methods were 92.49% and 95.67% respectively. The Monte Carlo method can be improved by analysing the less dense regions and then adapting the generation of points as seen in the study by Peidr o et al. [19].

A tighter boundary wrapping with a shrink factor of 1 was used for the discretization method as it provided better approximations. A shrink factor of 0.4 was used for the Monte Carlo method as it accommodated the randomness of the points and provided more suitable approximations. A shrink factor of 0.4 used for the discretization with an increment value of 5 caused the area value to be larger than the geometric method which is not physically possible. Therefore, a tighter wrapping was adopted for discretization.

Voids within the workspace complicate the workspace generation. Mechanical constraints must be considered and inequalities must be developed to reject invalid points. Overall, three methods were used to successfully generate the workspace for a 3RRR PKM with two of these methods providing suitable approximations of the workspace. The contribution of this paper was the comparison of each method together with its merits and drawbacks. Future work could include boundary refining methods and density compensation concerning the Monte Carlo method.

References

1. Z. Pandilov, and V. Dukovski, " Comparison of The Characteristics between Serial and Parallel Robots," *Acta Technica Corviniensis – Bulletin of Engineering*, vol. 7, no. 1, pp. 143-160, 2014.
2. J. M. Escorcia-Hern andez, A. Chemori, and H. Aguilar-Sierra, "Adaptive RISE Feedback Control for Robotized Machining with PKMs: Design and Real-Time Experiments," *IEEE Transactions on Control Systems Technology*, vol. 31, no. 1, pp. 39-54, 2023, doi: 10.1109/TCST.2022.3169015.
3. A. Peidr o, O. Reinoso, A. Gil, J. M. Mar n, L. Pay a, and Y. Berenguer, "Calculation of the Boundaries and Barriers of the Workspace of a Redundant Serial-parallel Robot using the Inverse Kinematics," in *ICINCO (2)*, 2016, pp. 412-420.
4. J.-P. Merlet, *Parallel Robots*, 2nd Edition ed. Springer Science & Business Media, 2006.
5. N. Le and X. H. Le, "Geometrical Design of a RUU Type Delta Robot Based on the Prescribed Workspace," in 2018 4th International Conference on Green Technology and Sustainable Development (GTSD), 23-24 Nov. 2018 2018, pp. 359-364, doi: 10.1109/GTSD.2018.8595674.
6. W. Li and J. Angeles, "A Novel Three-Loop Parallel Robot With Full Mobility: Kinematics, Singularity, Workspace, and Dexterity Analysis," *Journal of Mechanisms and Robotics*, vol. 9, no. 5, 2017, doi: 10.1115/1.4037112.
7. L. Moldovan, "Geometrical Method for Description of the 6-PGK Parallel Robot's Workspace," in 2008 First International Conference on Complexity and Intelligence of

- the Artificial and Natural Complex Systems. Medical Applications of the Complex Systems. Biomedical Computing, 8-10 Nov. 2008 2008, pp. 45-51, doi: 10.1109/CANS.2008.13.
8. S. Ay, A. Hacıoglu, and E. Vatandas, "A novel geometrical approach to determining the workspace of 6-3 Stewart Platform Mechanism," in Proceedings of 5th International Conference on Recent Advances in Space Technologies - RAST2011, 9-11 June 2011 2011, pp. 95-100, doi: 10.1109/RAST.2011.5966982.
 9. J.-P. Merlet, C. M. Gosselin, and N. Mouly, "Workspaces of planar parallel manipulators," *Mechanism and Machine Theory*, vol. 33, no. 1, pp. 7-20, 1998/01/01/ 1998, doi: [https://doi.org/10.1016/S0094-114X\(97\)00025-6](https://doi.org/10.1016/S0094-114X(97)00025-6).
 10. A. Yu, I. A. Bonev, and P. Zsombor-Murray, "Geometric approach to the accuracy analysis of a class of 3-DOF planar parallel robots," *Mechanism and Machine Theory*, vol. 43, no. 3, pp. 364-375, 2008/03/01/ 2008, doi: <https://doi.org/10.1016/j.mechmachtheory.2007.03.002>.
 11. B. Monsarrat and C. M. Gosselin, "Workspace analysis and optimal design of a 3-leg 6-DOF parallel platform mechanism," *IEEE Transactions on Robotics and Automation*, vol. 19, no. 6, pp. 954-966, 2003, doi: 10.1109/TRA.2003.819603.
 12. Y. Lou, G. Liu, and Z. Li, "Randomized Optimal Design of Parallel Manipulators," *IEEE Transactions on Automation Science and Engineering*, vol. 5, no. 2, pp. 223-233, 2008, doi: 10.1109/TASE.2007.909446.
 13. M. Russo and M. Ceccarelli, "A Comparison of Algebraic and Iterative Procedures for the Generation of the Workspace of Parallel Robots," in *Mechanism Design for Robotics*, Cham, S. Zeghloul, M. A. Laribi, and M. Arsicault, Eds., 2021// 2021: Springer International Publishing, pp. 53-61.
 14. S. D. Stan, M. Manic, C. Szep, and R. Balan, "Performance analysis of 3 DOF Delta parallel robot," in 2011 4th International Conference on Human System Interactions, HSI 2011, 19-21 May 2011 2011, pp. 215-220, doi: 10.1109/HSI.2011.5937369.
 15. E. Kuznetcova, V. Titov, E. Smirnov, I. Dalyaev, and A. Truts, "Design and Simulation Analysis of Haptic Device with Parallel Kinematic," vol. 29, 2018.
 16. A. N. Chaudhury and A. Ghosal, "Optimum design of multi-degree-of-freedom closed-loop mechanisms and parallel manipulators for a prescribed workspace using Monte Carlo method," *Mechanism and Machine Theory*, vol. 118, pp. 115-138, 2017/12/01/ 2017, doi: <https://doi.org/10.1016/j.mechmachtheory.2017.07.021>.
 17. A. Kosinska, M. Galicki, and K. Kedzior, "Designing and optimization of parameters of delta-4 parallel manipulator for a given workspace," *Journal of Robotic Systems*, vol. 20, no. 9, pp. 539-548, 2003.
 18. Y. Jianjun, S. Xiaojie, Z. Shiqi, Y. Ming, and Z. Xiaodong, "Monte Carlo method for searching functional workspace of an underwater manipulator," in 2018 Chinese Control And Decision Conference (CCDC), 9-11 June 2018 2018, pp. 6431-6435, doi: 10.1109/CCDC.2018.8408260.
 19. A. Peidr ,  . Reinoso, A. Gil, J. M. Mar n, and L. Pay , "An improved Monte Carlo method based on Gaussian growth to calculate the workspace of robots," *Engineering Applications of Artificial Intelligence*, vol. 64, pp. 197-207, 2017/09/01/ 2017, doi: <https://doi.org/10.1016/j.engappai.2017.06.009>.
 20. C. Gosselin and J. Angeles, "The Optimum Kinematic Design of a Planar Three-Degree-of-Freedom Parallel Manipulator," *Journal of Mechanisms, Transmissions, and Automation in Design*, vol. 110, no. 1, pp. 35-41, 1988, doi: 10.1115/1.3258901.